Observer-Based Secure Predefined-Time Control of Vehicular Platoon Systems Under Attacks in Sensors and Actuators

Zhenyu Gao, *Member, IEEE*, Xiang Li, Zhongyang Wei, Wei Liu, Ge Guo, *Senior Member, IEEE*, and Shixi Wen, *Senior Member, IEEE*

***Abstract*— Sensor and actuator attacks can alter the truth values of vehicle states and control input through false data injection, leading to performance degradation. In this paper, secure control of vehicular platoon control systems (VPCS) subject to joint sensor-actuator attacks, and the unknown disturbances is investigated. First, a novel adaptive sensor fusion algorithm is designed to estimate the actual position with smaller fusion errors. Subsequently, a predefined-time extended state observer (PTESO) is further constructed based on the estimated position to recover the continuous-time states (i.e., velocity and acceleration) and disturbances accurately within a user-defined settling time. Then, a variable exponent predefined-time sliding mode controller (VPTSMC) with few design parameters is developed to guarantee the predefined-time stability of the platoon system, namely string stability and individual vehicle stability. Meanwhile, the singularity phenomenon is also avoided. Finally, a serious of simulations are carried out to show the effectiveness of the suggested control scheme.**

***Index Terms*— Vehicular platoon control system (VPCS), sensor fusion, sensor-actuator attacks, observer control, predefined-time control.**

I. Introduction

With the rapid development of vehicle-related technologies, such as vehicular ad hoc network (VANET) technology, vehicle onboard sensor technology, and so on, various connected and automated vehicles (CAVs) have sprung up, which makes vehicular platoon control, as typical applications of CAVs, a reality and brings a serious of superiorities, such as lower fuel consumption, improved road traffic throughput, and enhanced road safety [1], [2], [3], [4], [5], [6], [7]. In order to achieve autonomous driving, compared with human-driven vehicles, CAVs are equipped with numerous sensors to obtain the necessary information, such as motion states, environment, etc., thus, the accuracy of sensors directly determines the secure control. However, sensors of CAVs lack the appropriate protection and are vulnerable to malicious cyber-attacks, leading to severe consequences or fatalities in the worst case [8], [9]. In addition, actuator attacks are often encountered for CAVs, which may cause an increase in engine revolutions or a damage of the braking, resulting in accidents [10]. Therefore, improving the tolerance to sensor-actuator attacks for a CAV is essential.

For the sensor attacks, sensor redundancy strategy is regarded as an effective way to enhance sensor measurement reliability, which have received great attention [11]. In such strategy, there are mainly two methods: set search algorithms which is applied for the case that the attacked set remains constant [12], [13], and sensor fusion algorithms which is effective for the uncertain attack set [14], [15]. With the increasing number of sensors, the attacker can attack different sensor by switching target, resulting an uncertain attacked set, thus, designing a more secure sensor fusion algorithm is the focus of current research. In [16], a sensor fusion algorithm was designed, achieving secure position state estimation by obtaining the median, while getting a larger fusion error when multiple sensors are attacked by the same sign. In [17], the most conservative security set can be obtained under the suggested fusion algorithm, to ensure that the estimated position state is not attacked but more noise information is lost. In [18], an adaptive sensor fusion algorithm was designed to estimate the security position state accurately, while reducing the influence of noise. However, to get better estimation accuracy, the adaptive parameter in [18] need to be adjusted according to the attack amplitude, which greatly reduces its applicability. This motivates the research in this paper to design a fusion algorithm that is more efficient and does not require parameters design to estimate the vehicle position information.

Noteworthy, the fusion output is discontinuous, making it unable for platoon continuous-time systems. Based on the characteristics of zero-order holder and filter, the technique of combining them is widely used for discrete-continuous state signal reconstruction to obtain smooth and continuous state values [19], [20]. However, both velocity and acceleration may change dramatically in a short time, resulting in large errors between discrete value and continuous one under the above method, which seriously reduces the accuracy of

Received 1 July 2024; revised 10 November 2024; accepted 7 February 2025. Date of publication 20 February 2025; date of current version 2 June 2025. This work was supported in part by the National Natural Science Foundation of China under Grant 62303101 and in part by the Natural Science Foundation of Hebei Province under Grant F2023501001. The Associate Editor for this article was S. Santini. *(Corresponding author: Zhenyu Gao.)*

Zhenyu Gao, Xiang Li, Zhongyang Wei, and Wei Liu are with the School of Control Engineering, Northeastern University at Qinhuangdao, Qinhuangdao 066004, China (e-mail: 18840839109@163.com; 2937795670@qq.com; 15953603659@163.com; liu_w1999@163.com).

Ge Guo is with the State Key Laboratory of Synthetical Automation for Process Industries, Northeastern University, Shenyang 110819, China (e-mail: geguo@yeah.net).

Shixi Wen is with the School of Information and Engineering, Dalian University, Dalian 116622, China (e-mail: 05423229@163.com).

Digital Object Identifier 10.1109/TITS.2025.3541240

signal reconstruction. To obtain continuous values of velocity and acceleration, the state observer technique was adopted by many researchers [21], [22], [23]. However, due to the existence of external disturbance and model uncertainties (i.e., parameter uncertainty, unmodeled dynamics, etc.), the conventional observer techniques are no longer applicable. In [24] and [25], the states of vehicles were estimated by extended state observers (ESOs), while adaptive techniques were employed to estimate the uncertainties. Recently, some improved ESOs were developed [26], [27], [28], [29], based on which the unknown states can be estimated with higher convergence rate. More specifically, in [28], an extended state observer based on a fractional order faster nonsingular terminal sliding mode control (SMC) scheme is proposed to simultaneously estimate velocity and disturbance for the problem of inaccurate velocity measurements in fast distributed platoon control. In [29], a fixed-time extended state observer (FxTESO) is designed to estimate the unknown state caused by the communication failure, external disturbances and parameter uncertainties of the vehicle platooning system, so as to achieve the platoon stability. However, the above design results are also not optimal in terms of convergence rate, while ignoring the effect of actuator attacks, which motivates the current study.

Convergence rate is also an important index to reflect the control performance of the VPCS, which has been widely studied [30], [31], [32]. For now, to improve the convergence speed, two main methods based on sliding mode control have been proposed, including finite-time control scheme [33] and fixed-time control algorithm [34], based on which, the tracking errors can be guaranteed to converge to the neighborhood near zero in finite time. Meanwhile, the fixed-time algorithm given in [34] also eliminates the strict constraint that settling time depends on the initial conditions of the system. However, there is one shortcoming that must be mentioned, i.e., the convergence time in [33] and [34] is a complicated function related to the designed control parameters, which makes it not easy to design and adjust parameters to meet the demands of the practical system. In addition, as described in [34], each parameter has a different effect on system performance, and the unreasonable selection of the control parameters will result in a larger convergence time or poor tracking accuracy. Lately, in [35], a novel SMC method based on predefined-time technique was designed for VPCS, wherein the convergence time can be predefined in advance and is independent of the control parameters. As most existing results, the singular phenomenon in [35] is often solved by designing a switching structure, which increases the complexity of controller, and the convergence rate still needs to be improved.

Based on the above analysis, the problem of vehicular platoon control with sensor attack, actuator attack, uncertain parameters and disturbances is investigated. An adaptive sensor fusion algorithm is designed to eliminate the influence of sensor attack, and then the disturbances, actuator attacks and the unknown states are obtained through the predefined-time extended state observer. A variable exponent predefined-time sliding mode controller is designed to make the vehicles achieve individual vehicle stability and string stability. The main contributions of this paper can be summarized as follows:

1) To obtain the attacked position information, a novel adaptive sensor fusion algorithm is designed. Compared to the method in [16], which calculates the median using all available data, and the method in [17], which utilizes only half of the data, the proposed algorithm utilizes as much secure data as possible to estimate position information while excluding attacked data, thus a smaller fusion error can be obtained. Besides, unlike the adaptive algorithm in [18], the given fusion algorithm does not need parameter settings, enhancing its applicability.
2) A predefined-time extended state observer (PTESO) is designed to simultaneously provide an estimate of the disturbances, actuator attacks and the unknown states. In contrast to the typical finite/fixed-time extended state observers [28], [29], the proposed PTESO cannot only guarantee the observer errors converge to zero within predefined time but also eliminate the restriction that the estimation time depend on the parameter design.
3) Based on the estimates of the PTESO, a novel variable exponent predefined-time tracking controller with superior performance is formulated for the heterogeneous vehicular platoon system, based on which predefined-time stability of the platoon system can be achieved. In addition, the "singularity phenomenon"is also avoided in this paper with few controller parameters than the SMCs in [34] and [35] that used the switched structure technique to overcome "singularity phenomenon", with obtaining a faster convergence rate than the finite-time SMC [30], [31], [32], [33] and fixed-time SMC [34], [35].

The structure of the remaining sections of this paper is as follows. In section II, preliminaries and problem formulation are presented. Section III gives the main results, including adaptive sensor fusion alsorithm design, predefined-time ESO design, predefined-time platoon tracking controller design and stability analysis. Simulation studies and conclusions are illustrated in Section IV and V, respectively.

II. Preliminaries and Problem Formulation

A. Preliminaries

In this subsection, we review some useful lemmas which will serve as the basis of the coming controller design and performance analysis.

Consider the following ordinary differential equation:

$$\dot{x}(t) = f(x(t)), x(0) = x_0 \tag{1}$$

with f is a continuous function such that $f(0) = 0$.

Lemma 1 [36]: If there exist a positive-definite Lyapunov candidate $V : \Re^n \to \Re^+$, and satisfies

$$\dot{V}(x) \leqslant -aV(x)^\gamma - bV(x)^\varpi \tag{2}$$

where $x \in \Re^n$, $a > 0$, $b > 0$, and $0 < \gamma < 1 < \varpi$, then system (1) is predefined-time stable and the settling-time satisfies

$$T(x_0) \leqslant \frac{1}{a(1-\gamma)} + \frac{1}{b(\varpi - 1)}. \tag{3}$$

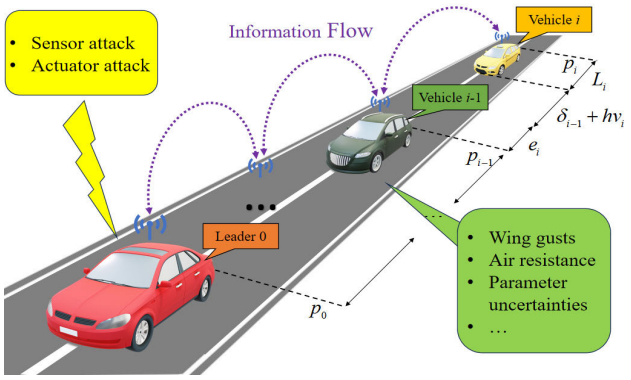

Fig. 1. The heterogeneous vehicular platoon system considered in this paper.

The predefined time $T_1(x_0)$ can be calculated by setting the parameters as follows

$$a = \frac{1}{(1-\gamma)\iota T(x_0)}, b = \frac{1}{(\varpi-1)(1-\iota)T(x_0)} \tag{4}$$

where ι is a positive and $\iota \in (0,1)$, $T_1(x_0)$ as a predefined convergence time can be given directly, neither constrained by the initial value nor dependent on the parameters design [36].

Lemma 2 [37]: For a system (1), if there exists a positive definite function $V(x)$ such that

$$\dot{V}(x) \leqslant -a_1 V(x)^{\gamma} - b_1 V(x)^{\varpi} + \eta \tag{5}$$

where $a_1 > 0$, $b_1 > 0$, and $0 < \gamma < 1 < \varpi$, then system (1) is fixed-time stable and the settling-time satisfies

$$T_1(x_0) \leqslant \frac{1}{a_1\varepsilon(1-\gamma)} + \frac{1}{b_1\varepsilon(\varpi-1)} \tag{6}$$

where $0 < \varepsilon < 1$ and the residual set of the solution for the system is obtained as

$$x \in \left\{\Omega(x) \leq \min\left\{\left(\frac{\eta}{(1-\varepsilon)a_1}\right)^{\frac{1}{\gamma}}, \left(\frac{\eta}{(1-\varepsilon)b_1}\right)^{\frac{1}{\varpi}}\right\}\right\}. \tag{7}$$

Based on Lemma 1, the system will converge to the set $\Omega(x)$ in a predefined time $T_1(x_0)$ if the parameters in (4) are set to $a = \frac{1}{(1-\gamma)\iota T_1(x_0)\varepsilon}$ and $b_1 = \frac{1}{(\varpi-1)(1-\iota)T_1(x_0)\varepsilon}$.

Lemma 3 [38]: Consider the function $f(x_1, x_2, \cdots, x_i) \in C\left(\Re^i, \Re\right), 1 \leqslant i \leqslant n$, if the Hlder continuous condition is satisfied then exists

$$|f(x_1, x_2, \cdots, x_i) - f(y_1, y_2, \cdots, y_i)| \leqslant \Psi \sum_{m=2}^{n} |x_m - y_m|^{\rho_{mi}} \tag{8}$$

where Ψ is a positive constant and $0 < \rho_{mi} \leqslant 1, i = 1, \cdots, n, m = 1, \cdots, i$.

B. Vehicle Dynamics

As shown in Fig. 1, a bidirectional (BD) topology-based vehicular platoon system with $N+1$ vehicles is considered in this paper, wherein the vehicle (labeled 0) denotes the leader to provide the desired platoon trajectory, and the vehicle i $(i \in 1, 2, \cdots, N)$ represents the following vehicle. Taking into account both unmodeled dynamics and unknown disturbances, the dynamics of following vehicle i is modeled as:

$$\begin{aligned} \dot{p}_i(t) &= v_i(t) \\ \dot{v}_i(t) &= a_i(t) \\ \dot{a}_i(t) &= f_i(v_i, a_i, t) + u_i + d_i(t) \end{aligned} \tag{9}$$

with

$$\begin{aligned} f_i(v_i, a_i, t) = -\frac{1}{m_i\tau_i}\Big[\rho_a A_i C_{ai}\left(\frac{1}{2}v_i^2 + \tau_i v_i a_i\right) \\ + m_i g b_i \cos\delta_i + m_i g \sin\delta_i\Big] - \frac{1}{\tau_i}a_i \end{aligned} \tag{10}$$

where $p_i(t)$, $v_i(t)$, $a_i(t)$ denote the position, velocity and acceleration of ith vehicle, respectively, $f_i(v_i, a_i, t)$ denotes uncertain unmodeled dynamics, and the definitions of other parameters can be found in Table I. Here, the leader dynamics is $\dot{p}_0(t) = v_0(t)$, $\dot{v}_0(t) = a_0(t)$, which is secure and attack-free.

Remark 1: Nowadays, the communication structures are mainly divided into six types: Predecessor-Following (PF), Predecessor-Leader-Following (PLF), Two Predecessor-Following (TPF), Bidirectional (BD), Bidirectional-Leader (BDL) and Two Predecessor-Leader Following (TPLF) [39]. Among them, the BD architecture cannot only guarantee the string stability but also reduce communication time delay (detailed analysis refer to [40]), which makes BD topology the most widely used communication structure at present [6], [32], [34], [35].

As in [41], $f_i(v_i, a_i, t)$ is decomposed into the following two terms:

$$f_i(v_i, a_i, t) = f_{i0}(v_i, a_i, t) + \Delta f_i(v_i, a_i, t) \tag{11}$$

where $f_{i0}(v_i, a_i, t)$ and $\Delta f_i(v_i, a_i, t)$ represent the known term and the uncertain term, respectively.

Here, the FDI attack acting on actuators and sensors are considered, and control input and state information are further modeled as:

$$\begin{cases} u_i = u_{0i} + \Delta u_{ui} \\ \Delta u_{ui} = \Lambda_{ui} \cdot \psi_{ui}(t) \end{cases} \tag{12a}$$

$$\begin{cases} *_{atki} = *_i + \Delta *_{si} \\ \Delta *_{si} = \Lambda_{*i} \cdot \psi_{*i}(t), \end{cases} \quad * = p, v, a \tag{12b}$$

with

$$\Lambda_{ui} = \begin{cases} 1, & \text{attack for actuator} \\ 0, & \text{no attack for actuator} \end{cases}$$

TABLE I
THE DEFINITION OF EACH PARAMETER

Parameter	Description	Parameter	Description
m_i	Vehicle's mass	$w_i(t)$	External disturbances
ρ_a	Air density	δ_i	Road slope angle
C_{ai}	Drag coefficient	A_i	Frontal cross-area
u_i	Control input	τ_i	Engine time constant
g	Acceleration of gravity	b_i	Road resistance coefficient

$$\Lambda_{*i} = \begin{cases} 1, \text{attack for sensor} \\ 0, \text{no attack for sensor} \end{cases} \quad *=p,v,a \tag{13}$$

where Δu_{ui} and $\Delta *_{si}$ are the attack injection variables, $\psi_{ui}(t)$ and $\psi_{*i}(t)$ are the attack strategy variables.

In this work, n sensors are used to measure the position information $p_i(t)$, we have

$$\mathbb{P}_i(t_l) = \mathbb{C}_i p_i(t_l) + \mathbb{W}_i(t_l) + \Delta\mathbb{P}_{si}(t_l) \tag{14}$$

with $\mathbb{P}_i(t_l) = [\mathbf{p}_i, \cdots, \mathbf{p}_n]^T$ denote the set of collected position information at time t_l, $l \in N^+$, $\mathbb{C}_i = [1, \cdots, 1]^T \in \Re^n$, $\mathbb{W}_i(t_l) = [\omega_{i1}, \cdots, \omega_{in}]^T$ denote the sensor measurement noise, $\Delta\mathbb{P}_{si}(t_l) = [\Delta p_{si1}, \ldots, \Delta p_{sin}]^T$ is the position sensor attack vector.

The following assumptions are given to facilitate our design.

Assumption 1 ([42], [43]): The disturbance d_i and its first derivative are bounded and satisfy $|d_i| \leq \bar{d}_i$ and $|\dot{d}_i| \leq \bar{\bar{d}}_i$ with $\bar{d}_i$ is an unknonw positive constant and $\bar{\bar{d}}_i$ is known. In addition, the measurement noise $\omega_{i,p}, (p = 1, 2, \cdots, n)$ satisfies $|\omega_{i,p}| \leqslant \bar{\omega}_i$ for all $t > 0$, where $\bar{\omega}_i$ is an unknown positive constant.

Assumption 2 ([16], [17]): The attack vector $\Delta p_{si}(t_l)$ has less than $n/2$ nonzero elements for any t_l.

Assumption 3: The time that both sensors (i.e., the velocity sensor and acceleration sensor) are attacked satisfies $t_{\Lambda_{*i}=1} < t_{\Lambda_{*i}=0}, * = v, a$.

Assumption 4: The function $f_{i0}(v_i, a_i, t)$ satisfies Hlder continuous condition.

Remark 2: In practice, the disturbance cannot be infinite within a certain range, thus Assumption 1 is reasonable. By configuring different types of position sensors, such as ultrasonic sonar, GPS, camera, LiDARs and radar, Assumption 2 is easily guaranteed [11]. Moreover, the range of parameters such that the function $f_{i0}(v_i, a_i, t)$ satisfies Hlder continuous condition can be given by the range limit of the actual vehicle states. It can be obtained by taking the partial derivative of v_i, a_i when it degenerates to Lipschitz continuity.

Remark 3: Unlike the position sensors, the velocity and acceleration sensors are relatively resistant to be exposed in an attack environment [25], which leads to the fact that the time for both sensors to be attacked must be less than the time they are secure, thus Assumption 3 is reasonable.

Here, the constant time headway policy (CTHP) is adopted, based on which, the inter-vehicle spacing error is defined as:

$$e_i = p_{i-1} - p_i - L_i - h_i v_i - \Delta_i \tag{15}$$

where L_i is the length of the ith vehicle, h_i denotes the time headway and Δ_i represents inter-vehicle minimum safe distance.

C. Control Objectives

Considering the influence of actuator attacks, sensor attacks and external disturbances, a novel predefined-time security control method is designed to achieve the following goals:

1) Predefined-time individual vehicle stability: A desired spacing between adjacent vehicles can be maintained in a predefined time T_i $\left(\text{i.e., } \lim_{t \to T_i} e_i \to 0 \text{ and } e_i \approx 0 \text{ when } t \geq T_i\right)$.
2) Predefined-time string stability: The spacing tracking error e_i do not increase along the platoon after a predefined time T_i^{con}, that is

$$|G_i(s)| = \left|\frac{E_{i+1}(s)}{E_i(s)}\right| \leq 1, \text{when } t \geq T_i^{con} \tag{16}$$

where $E_i(s)$ represents the Laplace transform of $e_i(t)$.

III. Main Results

In this section, a novel adaptive sensor fusion algorithm shown as Algorithm 1 is introduced to mitigate the adverse effects of position sensor attacks, and a PTESO is combined to provide the estimations of unknown information, including velocity, acceleration and lumped disturbance. In the end, a PTSMC scheme is developed, based on which, the control objectives can be realized.

A. Adaptive Sensor Fusion Algorithm Design

As described before, both sensor noise and sensor attacks may impact the measurement accuracy of position information, thus an adaptive sensor fusion algorithm is proposed to estimate the real value of position information.

Defining the number of attack-free position sensors is expressed as m. Based on Assumption 2, the number of attack-free position sensors satisfies $m \geqslant \frac{n}{2}, m \in N^+$. The element coordinates in the array are obtained by GET($\bullet$) function. The function DEL($\bullet$) is used to delete an element from the array. MID($\bullet$), MEAN($\bullet$) and SIZE($\bullet$) are defined to take the median, average and number of the elements in array, respectively. MAX($\bullet$), MIN($\bullet$) are used to find the maximum and minimum values.

Algorithm 1 Adaptive Sensor Fusion Algorithm

Initialize Θ_i, $\bar{Y}_i$, $\bar{P}_l$, Λ_i, $\bar{\Lambda}_i$, $\mathbb{P}_i(t_l)$;
Time $t = t_l$;
Set $P_l \leftarrow \mathbb{P}_i(t_l)$, $mean = \text{MEAN}(P_l)$, $mid = \text{MID}(P_l)$;
$m_0 = \text{SIZE}(P_l)$, $m_1 = 1$;
while $m_0 \geqslant n/2$ **do**
  $mean = \text{MEAN}(P_l)$, $mid = \text{MID}(P_l)$;
  $\Theta_i(m_1) = |mean - mid|$;
  $\bar{Y}_i(m_1) = \text{MEAN}(P_l)$;
  $\bar{P}_l = \text{MAX}(|P_l - mid|)$;
  $\text{DEL}(P_l(\text{GET}(\bar{P}_l)))$;
end while
if $\Lambda_i > \bar{\Lambda}_i$ **then**
  $\hat{p}_i(t_l) = mid$;
else
  $\hat{p}_i(t_l) = \bar{Y}_i(\text{GET}(\text{MIN}(\Theta_i)))$;
end if
$l+ = 1$;

Theorem 1: Under Assumption 2, by initializing the Algorithm 1, the estimated value $\hat{p}_i(t_l)$ can be obtained from the sensor measurements $\mathbb{P}_i(t_l)$ in (14) subject to position sensor attacks and noise. Meanwhile the boundedness of the estimation error can be guaranteed, and satisfies $|\hat{p}_i(t_l) - p_i(t_l)| \leqslant 3\bar{\omega}_i$.

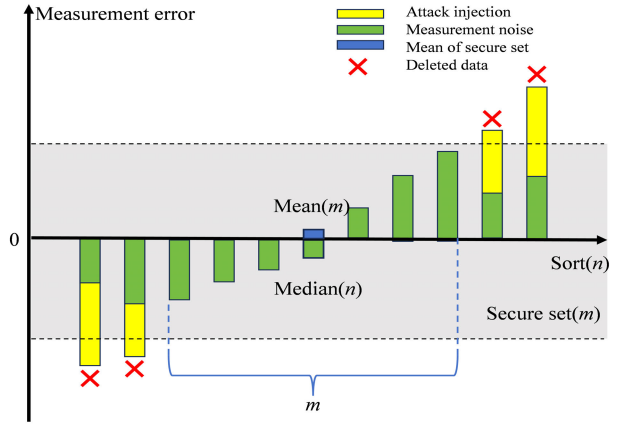

Fig. 2. Structure diagram of adaptive sensor fusion algorithm.

Proof: Based on Algorithm 1, we have

$$\text{MEAN}(P_l) = p_i(t_l) + \sum_{p=1}^{m_0} \frac{\omega_{i,p}}{m_0} + \sum_{p=1}^{m_0} \frac{\Delta\tilde{p}_{si,p}}{m_0} \tag{17}$$

and

$$\text{MID}(P_l) = p_i(t_l) + \omega_{i,mid} \tag{18}$$

where $\omega_{i,p}$, $\Delta\tilde{p}_{si,p}$ denote the noise and the attack injection variable of sensor p, respectively, and $\omega_{i,mid}$ are the noise on the median for vehicle i. Based on the fact that $|\sum_{p=1}^{m_0} \frac{\omega_{i,p}}{m_0}| \leqslant \bar{\omega}_i$ and $|\omega_{i,mid}| \leqslant \bar{\omega}_i$, then we have

$$|\Theta_i| = |\text{MEAN}(P_l) - \text{MID}(P_l)| \leqslant 2\bar{\omega}_i + \sum_{p=1}^{m_0} \frac{\Delta\tilde{p}_{si,p}}{m_0}. \tag{19}$$

When all attacked signals are deleted, the coordinates of the median set $\bar{Y}_i$ coincide with the coordinates of the minimum value in set Θ_i, and Θ_i satisfies $\Theta_i \leqslant 2\bar{\omega}_i$. In what follows, the proof is carried out by the following two cases. In case 1, $\hat{p}_i(t_l) = \text{MID}(P_l)$, so it is obtained that $|\hat{p}_i(t_l) - p_i(t_l)| \leqslant \bar{\omega}_i$ by (18). In case 2, according to $\hat{p}_i(t_l) = \text{MEAN}(P_l)$, then we have $|\hat{p}_i(t_l) - p_i(t_l)| \leqslant |\text{MID}(P_l) - p_i(t_l)| + \Theta_i \leqslant 3\bar{\omega}_i$.

Remark 4: Different from the median method adopted in [16], which is greatly affected by same-sign attacks. More conservative sensor fusion algorithm is proposed in [17], where discarding more data leads to sensor noise with a worse impact than the attacks. Moreover, the algorithm in [18] estimates the real information by adjusting the range of sensor data but the fusion estimation is more sensitive to the range change, and it is difficult to choose an appropriate parameter. As shown in Fig 2, it is obvious that for the proposed Algorithm 1, the difference between the median and mean of the data only needs to be as small as possible to ensure the accuracy of the estimation, thus, the difficulty of parameter selection is avoided. The numerical upper bound of the number about dropped data is guaranteed by $m_0 \geqslant n/2$. Λ_i is defined as a detection flag of the sensor fusion error, which will be given in the state observer design. When the attack causes the fusion error to exceed the threshold, a more conservative median value will be taken in Algorithm 1. In addition, the proposed algorithm (i.e., Algorithm 1) is also applicable to other measurement problems satisfying Assumption 1 and 2, such as sensor saturation, fault [44], network attack [45], etc.

B. Predefined-Time ESO Design

Based on Algorithm 1, the estimated value $\hat{p}_i(t_l)$ can be obtained, but it is in discrete form. For the subsequent design of the extended state observer, a continuous value of $\hat{p}_i(t_l)$ is needed, thus the following zero-order holder $H_{ZOH}(s)$ and second order butterworth low-pass filter $G_{LPF}(s)$ are introduced:

$$\begin{cases} H_{ZOH}(s) = \dfrac{1 - \mathbf{e}^{-sT_z}}{s} \\ G_{LPF}(s) = \dfrac{\omega_a^2}{s^2 + 1.414\omega_a + \omega_a^2} \end{cases} \tag{20}$$

where $\mathbf{e}$ is the base of the natural logarithm and ω_a denotes the cutoff frequency of $G_{LPF}(s)$.

Then a continuous form of position information can be obtained:

$$\hat{p}_i(t) = \hat{p}_i(t_l) H_{ZOH} G_{LPF}. \tag{21}$$

Considering both filtering error and the fusion error of Algorithm 1, thus one has

$$\Delta\hat{p}_{si}(t) = \hat{p}_i(t) - p_i(t). \tag{22}$$

Then, the dynamics of following vehicle can be written as:

$$\begin{aligned} \dot{\hat{p}}_i(t) &= v_i(t) + \Upsilon_i \\ \dot{v}_i(t) &= a_i(t) \\ \dot{a}_i(t) &= u_{0i}(t) + d_i + f_{0i}(v_i, a_i, t) \end{aligned} \tag{23}$$

where $\Upsilon_i = \Delta\dot{\hat{p}}_{si}$, and $d_i = \Delta f_i(v_i, a_i, t) + w_i + \Delta u_{ui}$ stands for the lumped disturbance acting on actuator of vehicle i.

Based on Theorem 1 and the definition of the derivative, there must exists an upper bound $\bar{\Upsilon}_i > 0$ such that $|\Upsilon_i| \leqslant \bar{\Upsilon}_i$. And it follows from (20) that $\ddot{\hat{p}}_i = \omega_a \hat{p}_i^2 - \omega_a^2 \hat{p}_i - 1.414\omega_a \dot{\hat{p}}_i$, so there exists a positive constant $\bar{\bar{\Upsilon}}_i$ such that $|\dot{\Upsilon}_i| \leqslant \bar{\bar{\Upsilon}}_i$.

Defining $z_{i,1} = \hat{p}_i$, $z_{i,2} = v_i$, $z_{i,3} = a_i$, $z_{i,4} = d_i$, and $\hat{z}_{i,j}$ is the observed value of $z_{i,j}$ for $j = 1, 2, 3, 4$, a predefined-time extended state observer is further designed:

$$\begin{cases} \dot{\hat{z}}_{i,j} = \hat{z}_{i,j+1} + \dfrac{k_{i,j}\text{sig}^{\alpha_{i,j}}(\mu_i^4(z_{i,1} - \hat{z}_{i,1}))}{\mu_i^{4-j}} \\ \qquad + \dfrac{k_{i,j}\text{sig}^{\beta_{i,j}}(\mu_i^4(z_{i,1} - \hat{z}_{i,1}))}{\mu_i^{4-j}}, j = 1, 2 \\ \dot{\hat{z}}_{i,j} = \hat{z}_{i,j+1} + u_{0i} + \dfrac{k_{i,j}\text{sig}^{\alpha_{i,j}}(\mu_i^4(z_{i,1} - \hat{z}_{i,1}))}{\mu_i^{4-j}} \\ \quad + \dfrac{k_{i,j}\text{sig}^{\beta_{i,j}}(\mu_i^4(z_{i,1} - \hat{z}_{i,1}))}{\mu_i^{4-j}} + f_{i0}(z_{i,1}, \cdots, \hat{z}_{i,j}), j = 3 \\ \dot{\hat{z}}_{i,j} = k_{i,j}\big(\text{sig}^{\alpha_{i,j}}(\mu_i^4(z_{i,1} - \hat{z}_{i,1})) \\ \qquad + \text{sig}^{\beta_{i,j}}(\mu_i^4(z_{i,1} - \hat{z}_{i,1}))\big), j = 4 \end{cases} \tag{24}$$

where $\alpha_{i,j} = j\rho_i - (j-1), \beta_{i,j} = -j\rho_i + (j+1), \rho_i \in (15/16, 1)$, μ_i is a positive constant, $k_{i,j}$ are selected, making L_i satisfies the Hurwitz matrix and there exists a symmetric positive definite P_i such that

$$L_i^T P_i + P_i L_i = -I_4 \tag{25}$$

with

$$L_i = \begin{bmatrix} -k_{i,1} & 1 & 0 & 0 \\ -k_{i,2} & 0 & 1 & 0 \\ -k_{i,3} & 0 & 0 & 1 \\ -k_{i,4} & 0 & 0 & 0 \end{bmatrix}.$$

Define $\vartheta_i(t) = [\vartheta_{i,1}, \vartheta_{i,2}, \vartheta_{i,3}, \vartheta_{i,4}]^T$ with $\vartheta_{i,j}(t) = \mu_i^{5-j}(z_{i,j}(t) - \hat{z}_{i,j}(t))$ for $j = 1, 2, 3, 4$, then the error system can be written as

$$\dot{\vartheta}_i(t) = F_i^1(t) + F_i^2(t) + F_i^3(t) \tag{26}$$

where $F_i^1(t) = \mu_i[\vartheta_{i,2}/2 - k_{i,1}\text{sig}^{\alpha_{i,1}}(\vartheta_{i,1}), \vartheta_{i,3}/2 - k_{i,2}\text{sig}^{\alpha_{i,2}}(\vartheta_{i,1}), \vartheta_{i,4}/2 - k_{i,3}\text{sig}^{\alpha_{i,3}}(\vartheta_{i,1}), -k_{i,4}\text{sig}^{\alpha_{i,4}}(\vartheta_{i,1})]^T$, $F_i^2(t) = \mu_i[\vartheta_{i,2}/2 - k_{i,1}\text{sig}^{\beta_{i,1}}(\vartheta_{i,1}), \vartheta_{i,3}/2 - k_{i,2}\text{sig}^{\beta_{i,2}}(\vartheta_{i,1}), \vartheta_{i,4}/2 - k_{i,3}\text{sig}^{\beta_{i,3}}(\vartheta_{i,1}), -k_{i,4}\text{sig}^{\beta_{i,4}}(\vartheta_{i,1})]^T$, and $F_i^3(t) = \mu_i^{5-j}[\Upsilon_i, 0, f_{i,0}(z_{i,1}, z_{i,2}, z_{i,3}) - f_{i,0}(z_{i,1}, \hat{z}_{i,2}, \hat{z}_{i,3}), \dot{d}_i]^T$.

To show the convergence of observer error, the following Lyapunov function is considered:

$$V_{Si}(\vartheta_i) = \vartheta_i^T P_i \vartheta_i. \tag{27}$$

Considering Assumption 4 and Theorem 1 in [46], the Lyapunov function convergence is satisfied

$$\begin{aligned} \dot{V}_{Si}(\vartheta_i) &\leqslant -\left(\Xi_i^1\mu_i - \Phi_i^1 - (|\Upsilon_i| + |\dot{d}_i|)\Gamma_i^1\right)V_{Si}^{\frac{(5-\rho_i)}{4}}, V_{Si} \geqslant 1 \\ \dot{V}_{Si}(\vartheta_i) &\leqslant -(\Xi_i^2\mu_i - \Phi_i^2 - (|\Upsilon_i| + |\dot{d}_i|)\Gamma_i^2)V_{Si}^{\frac{(3+\rho_i)}{4}}, V_{Si} \leqslant 1 \end{aligned} \tag{28}$$

with Ξ_i^1, Φ_i^1, Ξ_i^2, Φ_i^2, Γ_i^1 and Γ_i^2 are the positive parameters to be designed similar to that in [46]. Combining Assumption 1, we have

$$\begin{aligned} \dot{V}_{Si}(\vartheta_i) &\leqslant -\left(\Xi_i^1\mu_i - \Phi_i^1 - (\bar{\Upsilon}_i + \bar{\bar{d}}_i)\Gamma_i^1\right)V_{Si}^{\frac{(5-\rho_i)}{4}}, V_{Si} \geqslant 1 \\ \dot{V}_{Si}(\vartheta_i) &\leqslant -(\Xi_i^2\mu_i - \Phi_i^2 - (\bar{\Upsilon}_i + \bar{\bar{d}}_i)\Gamma_i^2)V_{Si}^{\frac{(3+\rho_i)}{4}}, V_{Si} \leqslant 1 \end{aligned} \tag{29}$$

Based on Lemma 1 and (29), Theorem 2 is given as follows.

Theorem 2: Consider the system (23) subject to Assumption 1. Under the extended state observer (24) with the gain vector (25), then the unknown states (i.e., velocity and acceleration) and the lumped disturbance can be observed accurately in predefined time, that is the extended state observer error ϑ_i will converge to zero within a predefined time T_i^S by setting μ_i as

$$\mu_i = \frac{4(\Xi_i^2 + \Xi_i^1)}{T_i^S\Xi_i^2(1-\rho_i)\Xi_i^1} + M_i \tag{30}$$

where $M_i = \min\left\{\frac{\Phi_i^1 + (\bar{\Upsilon}_i + \bar{\bar{d}}_i)\Gamma_i^1}{\Xi_i^1}, \frac{\Phi_i^2 + (\bar{\Upsilon}_i + \bar{\bar{d}}_i)\Gamma_i^2}{\Xi_i^2}\right\}$.

Proof: The convergence time for $V_{Si} \geqslant 1$ and $V_{Si} \leqslant 1$ are defined as $T_{1i}^S = \frac{\Xi_i^1}{\Xi_i^1 + \Xi_i^2}T_i^S$ and $T_{2i}^S = \frac{\Xi_i^2}{\Xi_i^2 + \Xi_i^1}T_i^S$., respectively. Based on Theorem 1 in [46], we have

$$\begin{aligned} \mu_i &= \frac{4}{T_{1i}^S(1-\rho_i)\Xi_i^1} + \frac{\Phi_i^1 + (\bar{\Upsilon}_i + \bar{\bar{d}}_i)\Gamma_i^1}{\Xi_i^1} \\ &= \frac{4}{T_{2i}^S(1-\rho_i)\Xi_i^2} + \frac{\Phi_i^2 + (\bar{\Upsilon}_i + \bar{\bar{d}}_i)\Gamma_i^2}{\Xi_i^2} \end{aligned} \tag{31}$$

thus, T_{2i}^S is denoted by

$$T_{2i}^S = \frac{4\Xi_i^1 T_{1i}^S}{4\Xi_i^2 + (M_{2i}\Xi_i^1 - M_{1i}\Xi_i^2)(1-\rho_i)T_{1i}^S} \tag{32}$$

with $M_{1i} = \Phi_i^1 + (\bar{\Upsilon}_i + \bar{\bar{d}}_i)\Gamma_i^1$, $M_{2i} = \Phi_i^2 + (\bar{\Upsilon}_i + \bar{\bar{d}}_i)\Gamma_i^2$.

By calculating, we have $T_{2i}^S \leq \frac{\Xi_i^1}{\Xi_i^2}T_{1i}^S$ when the condition $\frac{\Phi_i^1 + (\bar{\Upsilon}_i + \bar{\bar{d}}_i)\Gamma_i^1}{\Xi_i^1} \leq \frac{\Phi_i^2 + (\bar{\Upsilon}_i + \bar{\bar{d}}_i)\Gamma_i^2}{\Xi_i^2}$ is satisfied, and $T_{2i}^S \geq \frac{\Xi_i^1}{\Xi_i^2}T_{1i}^S$ on the contrary.

When μ_i is chosen as in (30), $T_{1i}^S + T_{2i}^S \leqslant T_i^S$ is satisfied, so ϑ_i will converge to zero within T_i^S. As mentioned in Remark 4 before, the following fusion error detection flag is adopted as $\Lambda_i = \left(z_{i,1}(cT_i^S) - \hat{z}_{i,1}(cT_i^S)\right) * H_{ZOH}(s), c \in N^+$. When $|\Upsilon_i| > \bar{\Upsilon}_i$, there exists a detection threshold $\bar{\Lambda}_i$ such that the detection flag $\Lambda_i > \bar{\Lambda}_i$.

Considering the velocity and acceleration sensor attacks and the influence of position sensor fusion error on the states estimated value, the following algorithm (i.e., Algorithm 2) is developed.

Algorithm 2 Velocity and Acceleration States Reconstruction Algorithm

Initialize Fix the detection threshold $\delta_{i,j}^d, j = 2, 3$;
while $t > 0$ **do**
  if $|z_{i,j}(t) - x_{*i,j}| \geqslant \delta_{i,j}^d$ **then**
    $\hat{x}_{i,j}(t) = z_{i,j}(t)$;
  else
    $\hat{x}_{i,j}(t) = x_{*i,j}(t)$;
  end if
end while

Remark 5: Considering the accuracy of the zero-order holder and second-order low-pass filter conversion, $T_z \leqslant T_i^F/2$ is set according to the Nyquist criterion, and T_p should be slightly larger than $2T_z$ to ensure an appropriate bandwidth. Moreover, since the velocity and acceleration sensors are relatively difficult to be exposed in the attack environment [47], it is reasonable that the reconstruction value in Algorithm 2 depends more on the measured value when the attack thresholds of velocity and acceleration sensor attacks are not reached.

C. Predefined-Time Platoon Tracking Controller Design

In this subsection, a novel variable exponent coefficient predefined-time sliding mode controller is designed to achieve the control objectives under attacks and external disturbances.

The sliding mode surface is designed as

$$S_i(t) = \dot{e}_i + \wp_i(e_i) + \bar{k}_{2i}e_i \tag{33}$$

with $\wp_i(e_i) = \bar{k}_{1i}|e_i|^{\bar{\alpha}_i e_i^{2\bar{v}}}\text{sign}(e_i)$, $\bar{k}_{1i} > 0$, $\bar{k}_{2i} > 0$, $\bar{\alpha}_i > 1$, $\bar{v} \in N^+$.

Here, to ensure predefined time individual vehicle stability and string stability of the platoon system, between the parameters $\bar{k}_{1i}$ and $\bar{k}_{2i}$, the following condition should be satisfied:

$$\bar{k}_{2i} = \lambda_i\bar{k}_{1i} \tag{34}$$

with

$$\lambda_i \geqslant \left[\bar{\alpha}_i^2 \mathbf{e}^{\frac{2-2\bar{v}}{\bar{v}}}\left(\mathbf{e}^{-\frac{1}{2\bar{v}}}-1\right)^2+2\bar{v}\bar{\alpha}_i\mathbf{e}^{\frac{1-\bar{v}}{\bar{v}}}\right]\mathbf{e}^{\frac{-\bar{\alpha}_i-\mathbf{e}}{2\bar{v}\mathbf{e}}} \tag{35}$$

and

$$\bar{k}_{1i}=\frac{1}{T_i^e(\bar{\alpha}_i-1)\bar{\gamma}_i}+\frac{1}{T_i^e\sqrt{2}\left(\mathbf{e}^{-\frac{\bar{\alpha}_i}{2\bar{v}\mathbf{e}}}\right)} \tag{36}$$

where $\bar{\gamma}_i=\max\left(2^{\frac{\bar{\alpha}_i+1}{2}},2\lambda_i\right)$, and T_i^e denotes the given settling time.

To guarantee the convergence of $S_i(t)$, taking the time derivative of $S_i(t)$ yields:

$$\dot{S}_i=\bar{k}_{1i}|e_i|^{\bar{\alpha}_i e_i^{2\bar{v}}}\left(\left(\bar{\alpha}_i e_i^{2\bar{v}-1}\right)\left(\operatorname{sign}(e_i)+2\bar{v}\ln(|e_i|)\right)\right)\dot{e}_i+\bar{k}_{2i}\dot{e}_i+\ddot{e}_i. \tag{37}$$

Remark 6: Note that the function $\vartheta: e_i \mapsto |e_i|^{\bar{\alpha}_i e_i^{2\bar{v}}}=\exp\left(\bar{\alpha}_i e_i^{2\bar{v}}\ln(|e_i|)\right)$ is continuous at $e_i=0$ with $\vartheta(0)=1$, and the function $\phi: e_i \mapsto e_i\ln(e_i)=0$ when $e_i=0$. So with the use of the proposed predefined-time variable exponent coefficient sliding mode surface (33), the singularity phenomenon is also avoided in this paper.

Then, based on (15) and (23), we can obtain $\dot{e}_i$ and $\ddot{e}_i$ as:

$$\dot{e}_i=v_{i-1}-\Upsilon_{i-1}-v_i+\Upsilon_i-h_i a_i \tag{38}$$

and

$$\ddot{e}_i=\ a_{i-1}-\dot{\Upsilon}_{i-1}-a_i+\dot{\Upsilon}_i-h_i(f_{0i}+u_{0i}+d_i). \tag{39}$$

As in [34] and [35], to ensure the string stability, the positive parameter $q, q\in(0,1]$ is adopted to couple $S_i(t)$ and $S_{i+1}(t)$:

$$\Pi_i(t)=\begin{cases} qS_i(t)-S_{i+1}(t), & i=1,2,\cdots,N-1\\ qS_i(t), & i=N.\end{cases} \tag{40}$$

Taking the time derivative of $\Pi_i(t)$ along (37) and (40) yields

$$\dot{\Pi}_i(t)=\begin{cases} q\left(-h_i u_{0i}+\Xi_{1i}+K(e_i)\Xi_{2i}-h_i d_i\right)+Z_i\\ \text{for } i=1,2,\cdots,N-1,\\ q(-h_i u_{0i}+\Xi_{1i}+K(e_i)\Xi_{2i}-h_i d_i)+Z_i\\ \text{for } i=N\end{cases} \tag{41}$$

with

$$Z_i=\begin{cases} q\left[-h_i f_{0i}+(a_{i-1}-a_i)+\left[\bar{k}_{2i}\right.\right.\\ \left.+\bar{k}_{1i}|e_i|^{\bar{\alpha}_i e_i^{2\bar{v}}}(\bar{\alpha}_i e_i^{2\bar{v}-1}(\operatorname{sign}(e_i)+\right.\\ \left.2\bar{v}\ln(|e_i|)))\right](v_{i-1}-v_i-h_i a_i)]-\dot{S}_{i+1}(t),\\ i=1,2,\cdots,N-1\\ q\left[-h_i f_{0i}+(a_{i-1}-a_i)+\left[\bar{k}_{2i}\right.\right.\\ \left.+\bar{k}_{1i}|e_i|^{\bar{\alpha}_i e_i^{2\bar{v}}}(\bar{\alpha}_i e_i^{2\bar{v}-1}(\operatorname{sign}(e_i)+\right.\\ \left.2\bar{v}\ln(|e_i|)))\right](v_{i-1}-v_i-h_i a_i)\right],\quad i=N\end{cases} \tag{42}$$

$$K(e_i)=\bar{k}_{1i}|e_i|^{\bar{\alpha}_i e_i^{2\bar{v}}}\left(\left(\bar{\alpha}_i e_i^{2\bar{v}-1}\right)\left(\operatorname{sign}(e_i)+2\bar{v}\ln(|e_i|)\right)\right)+\bar{k}_{2i} \tag{43}$$

and

$$\Xi_{1i}=\dot{\Upsilon}_i-\dot{\Upsilon}_{i-1} \tag{44}$$

$$\Xi_{2i}=\Upsilon_i-\Upsilon_{i-1} \tag{45}$$

where Ξ_{1i} and Ξ_{2i} stand for lumped errors and satisfy $|\Xi_{1i}|\leq\bar{\Xi}_{2i}$ and $|\Xi_{1i}|\leq\bar{\Xi}_{2i}$.

Combining with Lemma 1, the following reaching law is considered to guarantee the convergence of the proposed sliding mode surface (33):

$$\dot{\Pi}_i(t)=-\bar{K}_{1i}\operatorname{sig}^{\bar{\mu}_{1i}}(\Pi_i)-\bar{K}_{2i}\operatorname{sig}^{\bar{\mu}_{2i}}(\Pi_i) \tag{46}$$

where $0<\bar{\mu}_{1i}<1, \bar{\mu}_{2i}>1$, and both parameters $\bar{K}_{1i}$ and $\bar{K}_{2i}$ are chosen as

$$\bar{K}_{1i}=\frac{2^{\frac{1-\bar{\mu}_{1i}}{2}}}{\varepsilon_i(1-\bar{\mu}_{1i})\bar{\theta}_i T_i^{\Pi}},\bar{K}_{2i}=\frac{2^{\frac{1-\bar{\mu}_{2i}}{2}}}{\varepsilon_i(\bar{\mu}_{2i}-1)(1-\bar{\theta}_i)T_i^{\Pi}} \tag{47}$$

with $0<\varepsilon_i,\bar{\theta}_i<1$, and $T_i^{\Pi}>0$ denotes the predefined convergence time.

Substituting (46) into (37), the control input is designed as:

$$u_{0i}(t)=\frac{1}{qh_i}\left[\bar{K}_{1i}\operatorname{sig}^{\bar{\mu}_{1i}}(\Pi_i)+\bar{K}_{2i}\operatorname{sig}^{\bar{\mu}_{2i}}(\Pi_i)+\hat{Z}_i+qh_i\hat{d}_i\right] \tag{48}$$

where $\hat{Z}_i$ and $\hat{d}_i$ are the estimated values of Z_i and d_i by PTESO (24).

D. Stability Analysis

Theorem 3: Consider the vehicular platoon (9) subject to actuator attacks, sensor attacks and external disturbances (23), by designing PTESO (24), Algorithms 1 and 2, the proposed predefined-time control law (48) makes e_i converge to zero, i.e., the individual vehicle stability is ensured. Moreover, the string stability (16) also can be guaranteed.

The proof of Theorem 3 is accomplished through the following two parts.

1) Predefined-Time Individual Vehicle Stability: Consider the following Lyapunov function

$$V_{\Pi i}=\frac{1}{2}\Pi_i^2 \tag{49}$$

and taking the first time derivative of $V_{i\Pi}$ yields

$$\dot{V}_{\Pi i}=\Pi_i\dot{\Pi}_i=\Pi_i\left(q\dot{S}_i(t)-\dot{S}_{i+1}(t)\right). \tag{50}$$

Using the control law (48), we have

$$\dot{V}_{\Pi i}=\Pi_i(-\bar{K}_{1i}\operatorname{sig}^{\bar{\mu}_{1i}}(\Pi_i)-\bar{K}_{2i}\operatorname{sig}^{\bar{\mu}_{2i}}(\Pi_i)+q\Xi_{1i}+q\mathrm{K}(e_i)\Xi_{2i}-qh_i\tilde{d}_i). \tag{51}$$

Based on Theorem 1, one has $\tilde{d}_i\equiv 0$, when $t_i>T_i^S$ as long as appropriate observer parameters are chosen, then we have

$$\dot{V}_{\Pi i}\leq\Pi_i(-\bar{K}_{1i}\operatorname{sig}^{\bar{\mu}_{1i}}(\Pi_i)-\bar{K}_{2i}\operatorname{sig}^{\bar{\mu}_{2i}}(\Pi_i)+\eta_i\leq-\bar{K}_{1i}2^{\frac{\bar{\mu}_{1i}+1}{2}}V_{\Pi i}^{\frac{\bar{\mu}_{1i}+1}{2}}-\bar{K}_{2i}2^{\frac{\bar{\mu}_{2i}+1}{2}}V_{\Pi i}^{\frac{\bar{\mu}_{2i}+1}{2}}+\eta_i \tag{52}$$

where $\eta_i = q\bar{\Xi}_{1i} + q\bar{\Xi}_{2i}\max\{\bar{k}_{2i}, \mathrm{K}(e_{\max i})\}$, $e_{\max i}$ is the maximum value of tracking error.

Then, the convergence time T_i^C can be calculated as

$$T_i^C \leqslant T_i^{\Pi} + T_i^S. \tag{53}$$

Based on Lemma 2, when $t > T_i^C$, the corresponding sliding mode surface Π_i converges to the following small region Ω_i nearby the origin:

$$\Omega_i \leq \min\left\{\left(\frac{\eta_i}{(1-\varepsilon_i)\bar{K}_{1i}2^{\frac{\bar{\mu}_{1i}+1}{2}}}\right)^{\frac{2}{\bar{\mu}_{1i}+1}}, \left(\frac{\eta_i}{(1-\varepsilon_i)\bar{K}_{2i}2^{\frac{\bar{\mu}_{2i}+1}{2}}}\right)^{\frac{2}{\bar{\mu}_{2i}+1}}\right\}. \tag{54}$$

Once $\Pi_i \approx 0$ when $t > T_i^C$, owing to Π_i and S_i are equivalent, then the sliding mode surface S_i in (33) can be rewritten as

$$\dot{e}_i = -\bar{k}_{1i}|e_i|^{\bar{\alpha}_i e_i^{2\bar{v}}}\operatorname{sign}(e_i) - \bar{k}_{2i}e_i. \tag{55}$$

To proof the convergence of e_i, consider the Lyapunov function as follows:

$$V_{ei} = \frac{1}{2}e_i^2. \tag{56}$$

The whole analysis is given by the following two cases.

Case 1: when $|e_i| > 1$, with Eq.(36) we have

$$\begin{aligned}\dot{V}_{ei} &= -\bar{k}_{1i}|e_i|^{\bar{\alpha}_i e_i^{2\bar{v}}+1} - \bar{k}_{2i}|e_i|^2 \\ &\leqslant -\bar{k}_{1i}|e_i|^{\bar{\alpha}_i+1} - \bar{k}_{2i}|e_i|^2 \\ &\leqslant -\bar{k}_{1i}2^{\frac{\bar{\alpha}_i+1}{2}}V_{ei}^{\frac{\bar{\alpha}_i+1}{2}} - 2\bar{k}_{2i}V_{ei} \\ &\leqslant -\bar{\gamma}_i V_{ei}^{\frac{\bar{\alpha}_i+1}{2}}\end{aligned} \tag{57}$$

where the convergence time $T_{1i}^e = \frac{1}{\bar{k}_{1i}(\bar{\alpha}_i-1)\bar{\gamma}_i}$.

Case 2: if $|e_i| \leqslant 1$, $\dot{V}_{ei}$ satisfies

$$\begin{aligned}\dot{V}_{ei} &= -\bar{k}_{1i}|e_i||e_i|^{\bar{\alpha}_i e_i^{2\bar{v}}} - \bar{k}_{2i}|e_i|^2 \\ &\leqslant -\bar{k}_{1i}|e_i|\min(|e_i|^{\bar{\alpha}_i e_i^{2\bar{v}}}) \\ &\leqslant -\bar{k}_{1i}\sqrt{2}\mathbf{e}^{-\frac{\bar{\alpha}_i}{2\bar{v}\mathbf{e}}}V_{ei}^{\frac{1}{2}}\end{aligned} \tag{58}$$

where the second convergence time $T_{2i}^e = \frac{1}{\bar{k}_{1i}\sqrt{2}\left(\mathbf{e}^{-\frac{\bar{\alpha}_i}{2\bar{v}\mathbf{e}}}\right)}$. By designing parameters, such that e_i converges to zero in a predefined time $T_i^e = T_{1i}^e + T_{2i}^e$.

Through the above analysis, it is concluded that all the states (i.e., Π_i, S_i and e_i) are predefined-time stable, that is individual stability of the platoon, and the convergence time satisfies $T_i^{con} \leqslant T_i^C + T_i^e$.

2) Predefined-Time String Stability: The proof is along similar lines as in [18] and [30], where $|\wp_i(e_{i+1}) + \bar{k}_{i+1}e_{i+1}| \leq |\wp_i(e_i) + \bar{k}_i e_i|$ is required.

While $e_{i+1}(t) < e_i(t) < 0$, the function $\wp_i(e_i)$ in (33) is monotonically increasing on $e_i \in (-\infty, -\mathbf{e}^{-\frac{1}{2\bar{v}}}]$ and monotonically decreasing on $e_i \in (-\mathbf{e}^{-\frac{1}{2\bar{v}}}, 0)$. To make $\wp_i(e_i) + \bar{k}_i e_i$ monotonically decreasing on $e_i \in (-\infty, 0]$, we have

$$\bar{k}_{2i} \geq \dot{\wp}_i(\mathbf{e}^{-\frac{1}{2\bar{v}}}) - \ddot{\wp}_i(\mathbf{e}^{-\frac{1}{2\bar{v}}}) * \mathbf{e}^{-\frac{1}{2\bar{v}}} > -\min(\dot{\wp}_i(e_i)). \tag{59}$$

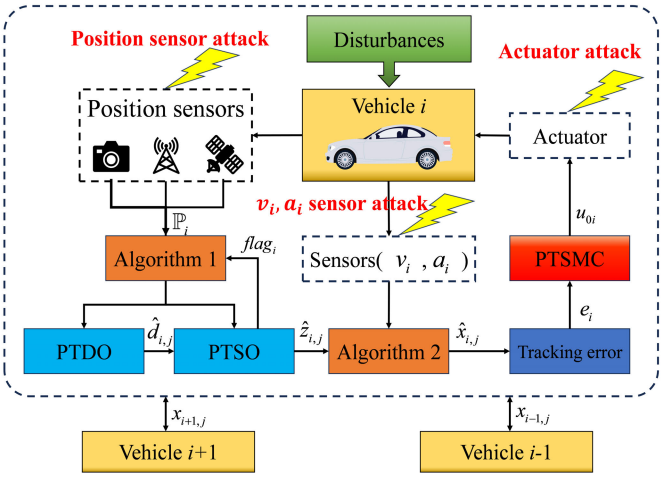

Fig. 3. Sketch of the proposed vehicle platoon control scheme.

TABLE II
RELATIONSHIP OF EACH PARAMETER WITH T_i^{con} AND Ω_i

$\bar{\mu}_{1,i}\uparrow$	$\bar{\mu}_{2,i}$	$T_{i,j}^{\Pi}$	$\bar{\theta}_i$	ε_i	T_i^e	T_i^{con}	$\Omega_i\uparrow$
$\bar{\mu}_{1,i}$	$\bar{\mu}_{2,i}\uparrow$	$T_{i,j}^{\Pi}$	$\bar{\theta}_i$	ε_i	T_i^e	T_i^{con}	$\Omega_i\downarrow$
$\bar{\mu}_{1,i}$	$\bar{\mu}_{2,i}$	$T_{i,j}^{\Pi}\uparrow$	$\bar{\theta}_i$	ε_i	T_i^e	$T_i^{con}\uparrow$	$\Omega_i\uparrow$
$\bar{\mu}_{1,i}$	$\bar{\mu}_{2,i}$	$T_{i,j}^{\Pi}$	$\bar{\theta}_i\uparrow$	ε_i	T_i^e	T_i^{con}	$\Omega_i\downarrow$
$\bar{\mu}_{1,i}$	$\bar{\mu}_{2,i}$	$T_{i,j}^{\Pi}$	$\bar{\theta}_i$	$\varepsilon_i\uparrow$	T_i^e	T_i^{con}	$\Omega_i\uparrow$
$\bar{\mu}_{1,i}$	$\bar{\mu}_{2,i}$	$T_{i,j}^{\Pi}$	$\bar{\theta}_i$	ε_i	$T_i^e\uparrow$	$T_i^{con}\uparrow$	Ω_i

There exists $e_i(t_0)$ such that $\dot{\wp}_i(e_i(t_0)) = 0$, we have

$$\begin{aligned}\bar{k}_{2i}^{\min} &= -\ddot{\wp}_i(e_i)(e_i(t_0)) \\ &= \left[\bar{\alpha}_i^2\mathbf{e}^{\frac{2-2\bar{v}}{\bar{v}}}\left(\mathbf{e}^{-\frac{1}{2\bar{v}}}-1\right)^2 + 2\bar{v}\bar{\alpha}_i\mathbf{e}^{\frac{1-\bar{v}}{\bar{v}}}\right]\mathbf{e}^{\frac{-\bar{\alpha}_i-\mathbf{e}}{2\bar{v}\mathbf{e}}}\bar{k}_{1i}.\end{aligned} \tag{60}$$

Based on $\ddot{\wp}_i(e_i) > 0$ and (59), such that

$$\bar{k}_{2i}^{\min} > -\min(\dot{\wp}_i(e_i)). \tag{61}$$

Hence, an appropriate choice of $\bar{k}_{2i}$ makes $\wp_i(e_i) + \bar{k}_{2i}e_i$ monotonically increasing in $e_i < 0$.

While $0 < e_i(t) < e_{i+1}(t)$, it is only needed to choose an appropriate $\bar{k}_{2i}$.

On the basis of the above analysis, it is obvious that when $t \geq T_i^{con}$, if $0 < q \leq 1$ and $\bar{k}_{2i} > \bar{k}_{2i}^{\min}$, predefined-time string stability can be guaranteed.

To make it clearer, the framework of the proposed control approach is given in Fig. 3. And for better performance, the parameter selection principle can be referred to Table II.

IV. Simulation Studies

In this section, numerical simulations which adopt a platoon of four vehicles and a leader ($i = 0, 1, 2, 3, 4$, where $i = 0$ stands for the leader) are carried out, by using the MATLAB/Simulink software, to demonstrate the effectiveness of the developed scheme. Here, the platoon parameters are selected as: $\Delta_i = 7m$, $h = 0.4s$, $g = 9.8m/s^2$, $\delta_i = 0$, $\Delta f_i(v_i, a_i, t) = 0.5 f_{i0}(v_i, a_i, t)$. Other parameters are given in Table III, and the initial states (i.e., positions

TABLE III
OTHER PARAMETERS FOR FOLLOWERS

Parameter \ Vehicle	1	2	3	4
$m_i(kg)$	1550	1600	1500	1450
$\tau_i(s)$	0.15	0.25	0.2	0.3
$L_i(m)$	3	3.5	3.2	2.9
C_{ai}	0.3	0.34	0.29	0.31
b_i	0.02	0.03	0.015	0.025
$\rho_{ai}(kg/m^3)$	1.2	1.1	1.3	1.0
$A_i(m^2)$	2.4	2.2	2.3	2.4

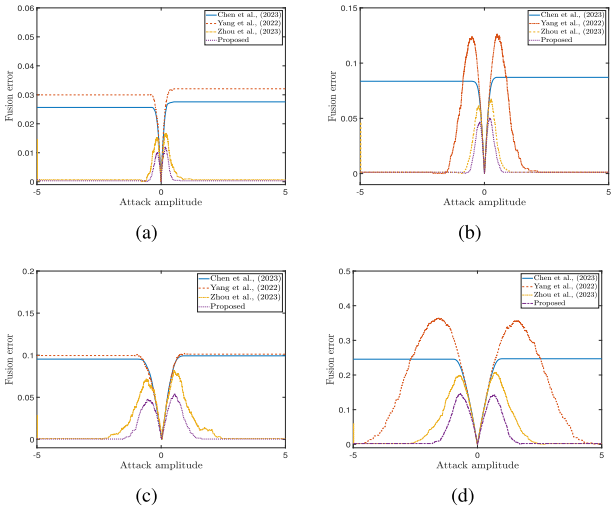

Fig. 4. Fusion error comparison results. (a) One attacked sensor under the Gaussian noise. (b) Two attacked sensors under the Gaussian noise. (c) One attacked sensor under the uniform random noise. (d) Two attacked sensors under the uniform random noise.

and velocities) of the followers are selected as: $p_i(0) = [109, 97, 85, 73.5, 62]\,m$, $v_i(0) = [0, 1, 1.2, 0.9, 0]m/s$ and $a_i(0) = 0\ m/s^2$. The actuator attack is set as $\psi_{ui}(t) = 3\mathbf{e}^{-(t-35)^2}\sin t$ and the external disturbance is set as $w_i(t) = \sin t$.

In order to test the control performance under different dynamics stages of the platooning vehicles, the acceleration of leader is designed as:

$$a_0(t) = \begin{cases} 0.5t\ m/s^2, & 0s \le t < 4s \\ 2\ m/s^2, & 4s \le t < 8s \\ -0.5t + 6\ m/s^2, & 8s \le t < 12s \\ 0\ m/s^2, & 12s \le t \le 50s. \end{cases} \tag{62}$$

A. The Performance of the Proposed Adaptive Sensor Fusion Algorithm

The performance of the proposed adaptive sensor fusion algorithm is examined in this section by comparing simulations. Consider five position sensors measuring a constant value of 100 meters, where one or two of these sensors are attacked, and the sensor noise is Gaussian noise $\omega_i = N \sim (0, 0.1)$ and uniform random noise $\omega_i = U \sim (-0.5, 0.5)$, respectively. The parameters of the adaptive sensor fusion algorithm in [18] are set as $\beta(0) = 2.2, \rho_d(0) = 0.01$, $\rho_u = 0.05$. The attack amplitude is from -5 to 5, and the Y-axis is the mean fusion error after 500 iterations under different distribution of noise.

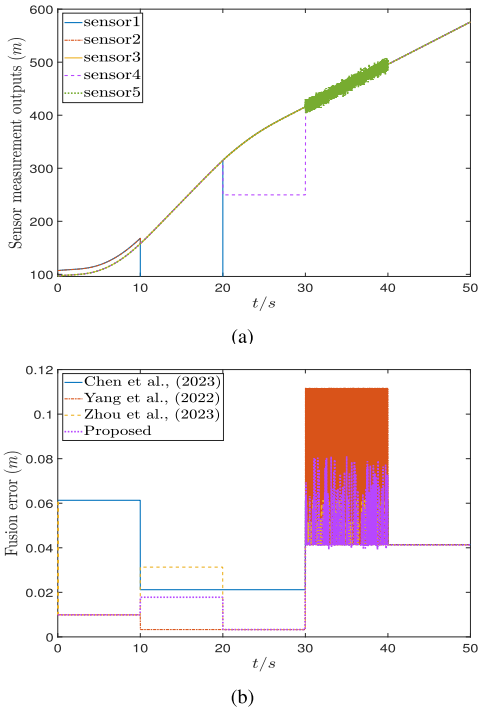

Fig. 5. The result of position sensor fusion. (a) The position sensor attack settings. (b) The fusion error.

The comparison results between the proposed algorithm and the fusion algorithms in [16], [17], and [18] are shown in Fig. 4. Compared with the algorithm in [16], the proposed algorithm has smaller fusion error when the attack amplitude is large (greater than $2\bar{\omega}_i$). As shown in (a), (c) in Fig. 4, the algorithm in [17] performs worse when the number of attacked sensors is less than $n/2$. The adaptive sensor fusion algorithm in [18] has a small fusion error, but the error increases in the beginning stage (when the attack amplitude is close to -5) in Fig. 4, which is due to the parameter settings that affect the fusion error in the adaptive stage. The proposed algorithm does not require the design of parameters and the number of attacked sensors to be known, and has smaller fusion error. The above analysis is consistent with that in Remark 2. Therefore, the proposed adaptive sensor fusion algorithm has better overall performance.

B. The Performance of the Predefined-Time Control Scheme

In this section, the position sensor attack settings are shown in Fig. 5(a) ($\Lambda_{pi} = 1, i = 1, 2, 3, 4$, taking follower 1 as an example). In the first stage, sensors 1 and 2 are attacked by a constant attack with $\Delta p_{si} = 10$; in the second stage, sensor 1 is damaged due to attack; in the third stage, sensor 4 is set to 250 (m); in the fourth stage, sensor 5 is attacked by noise injection $\Delta p_{si} = U \sim (-5, 5)$; and in the fifth stage, all sensors work normally. The fusion error is shown in Fig. 5(b), and the proposed adaptive sensor fusion algorithm maintains a low fusion error at each stage.

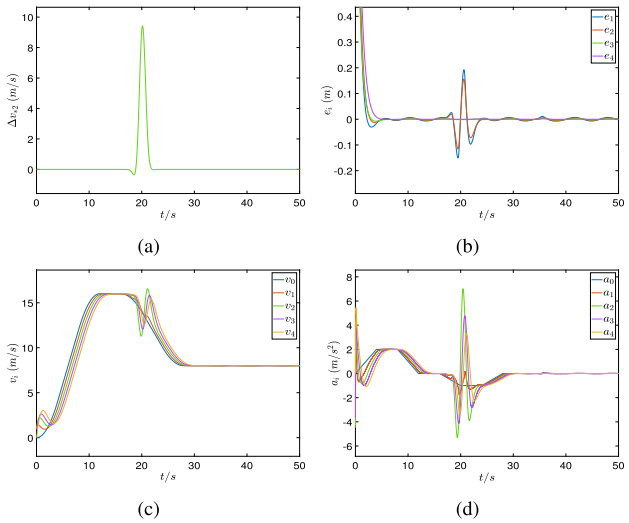

Fig. 6. Vehicle platoon under velocity sensor attack. (a) The attack injection variable. (b) Tracking error. (c) Velocity. (d) Acceleration.

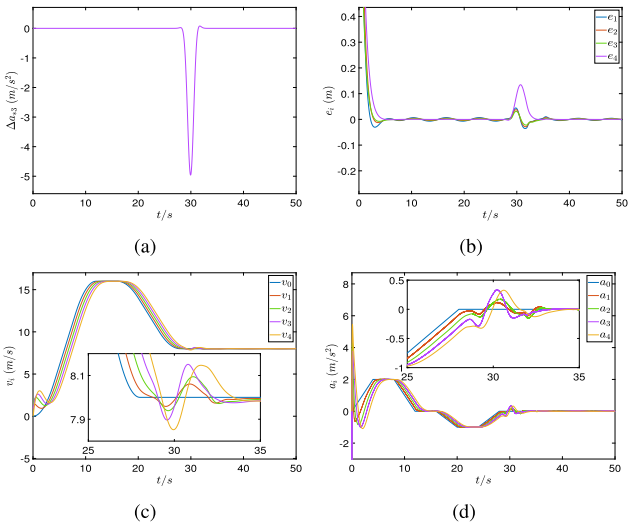

Fig. 7. Vehicle platoon under acceleration sensor attack. (a) The attack injection variable. (b) Tracking error. (c) Velocity. (d) Acceleration.

The velocity sensor attack and acceleration sensor attack are set to occur in vehicles 2 and 3, respectively. And the attack injection variables are $\Lambda_{v2} = 1$, $\psi_{vi}(t) = 10\mathbf{e}^{-(t-20)^2}\sin t$ and $\Lambda_{a3} = 1$, $\psi_{ai}(t) = 5\mathbf{e}^{-(t-30)^2}\sin t$. When the velocity sensor attack and acceleration sensor attack occurs, the simulation results of the vehicle platoon without Algorithm 2 are shown in Figs. 6 and 7.

From the simulation results in Figs. 6 and 7, it can be seen that the sensor and actuator attacks cause the performance degradation of the platoon. Although the attack variable only injected one vehicle, the states of all neighboring following vehicles are affected due to the connectivity of platoon. The velocity and acceleration chattering will adversely affect the traffic flow, and may even lead to pileup collisions.In order to achieve the safe control of the vehicle platoon, the parameters of proposed PTESO and VPTSMC are given in Table IV. Combined with Algorithm 1 and Algorithm 2, the simulation results are shown in Figs. 8 and 9.

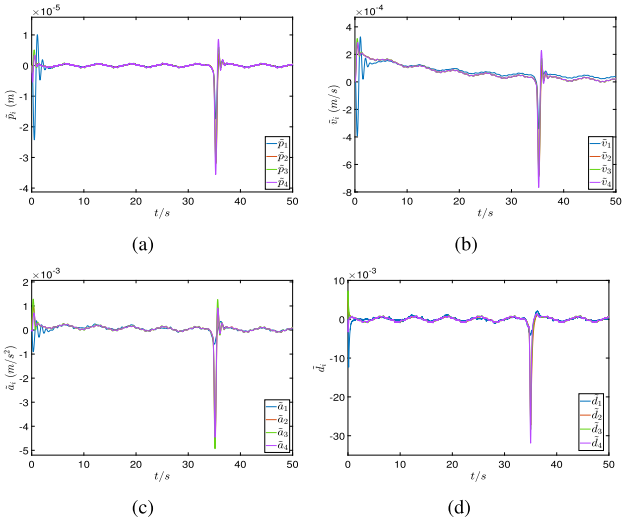

Fig. 8. Simulation results of the proposed PTESO. (a) The estimation error of p_i. (b) The estimation error of v_i. (c) The estimation error of a_i. (d) The estimation error of d_i.

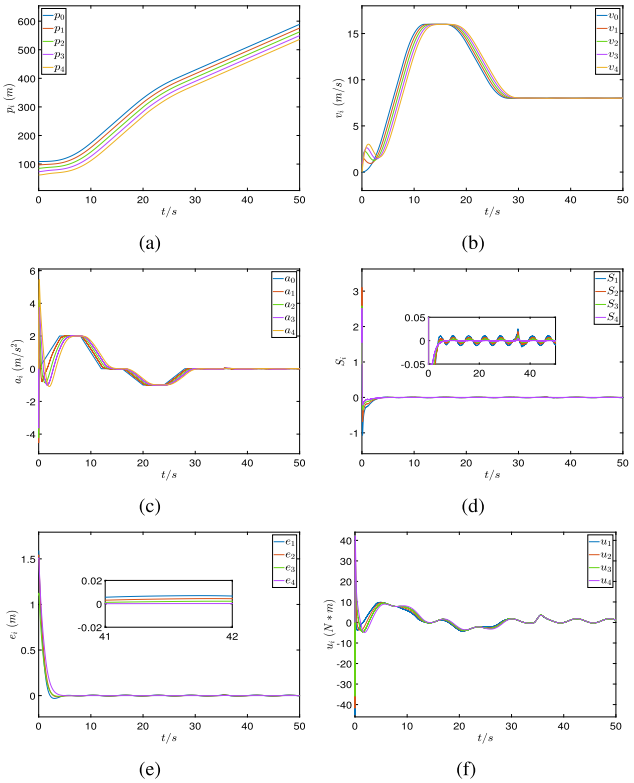

Fig. 9. Simulation results of the proposed VPTSMC. (a) Position. (b) Velocity. (c) Acceleration. (d) Sliding mode surface. (e) Tracking error. (f) Control input.

It can be seen from Fig. 8 that the designed PTESO can achieve the estimation of disturbances and states respectively within a predefined time. Due to the design of Algorithm 1 and Algorithm 2, it can be seen from Fig. 9(a), (b) and (c) that the states of the system are almost unaffected by the sensor injection attack, and the disturbances are actively eliminated combined with the estimated value of PTESO. Both (d), (e) of Fig. 9 indicate that the sliding surface and tracking error of the system converge in a predefined time, and the thumbnail of Fig. 9(e) shows that the string stability is achieved through the designed control scheme.

TABLE IV
PARAMETERS OF CONTROLLERS

Proposed method	Parameters
PTESO (24)	$\rho = 17/18, k_{i,j} = 2, T_{i,j}^{S} = 2s$
VPTSMC (48)	$\bar{\mu}_{1,i} = 3/5, \bar{\mu}_{2,i} = 5/3, T_{i,j}^{\Pi} = 3s, \bar{\theta}_i = \varepsilon_i = 0.1$ $T_i^e = 4s, \bar{\alpha}_i = 11/10, \bar{v} = 1$

V. CONCLUSION

In this paper, a secure predefined time sliding mode control scheme is proposed for vehicular platoon systems under the effect of sensor-actuator attacks and external disturbances. A novel adaptive sensor fusion algorithm with small fusion error and no design parameters is presented to against the position sensor sparse injection attack. A PTESO is developed for the unknown velocity, acceleration, actuator injection attack and lumped disturbance estimation simultaneously. In order to solve the singular phenomenon and improve the convergence rate, a novel variable exponent predefined-time sliding mode controller is designed, based on which both individual vehicle stability and string stability all can be guaranteed in predefined time. Here, the 1-D plane vehicular platoons is only considered, yet many application scenarios in reality are in the 2-D plane, such as tunnels, ramps, passing through construction sections, etc., thus future work is the secure control of 2-D plane vehicle platooning systems under sensor attacks.

REFERENCES

[1] S. Chu and A. Majumdar, "Opportunities and challenges for a sustainable energy future," *Nature*, vol. 488, no. 7411, pp. 294–303, Aug. 2012.

[2] D. Liu, S. Mair, K. Yang, S. Baldi, P. Frasca, and M. Althoff, "Resilience in platoons of cooperative heterogeneous vehicles: Self-organization strategies and provably-correct design," *IEEE Trans. Intell. Vehicles*, vol. 9, no. 1, pp. 2262–2275, Jan. 2024.

[3] A. Alam, B. Besselink, V. Turri, J. Mårtensson, and K. H. Johansson, "Heavy-duty vehicle platooning for sustainable freight transportation: A cooperative method to enhance safety and efficiency," *IEEE Control Syst. Mag.*, vol. 35, no. 6, pp. 34–56, Dec. 2015.

[4] H. Chehardoli and A. Ghasemi, "Adaptive centralized/decentralized control and identification of 1-D heterogeneous vehicular platoons based on constant time headway policy," *IEEE Trans. Intell. Transp. Syst.*, vol. 19, no. 10, pp. 3376–3386, Oct. 2018.

[5] J. Chen, H. Liang, J. Li, and Z. Lv, "Connected automated vehicle platoon control with input saturation and variable time headway strategy," *IEEE Trans. Intell. Transp. Syst.*, vol. 22, no. 8, pp. 4929–4940, Aug. 2021.

[6] J.-W. Kwon and D. Chwa, "Adaptive bidirectional platoon control using a coupled sliding mode control method," *IEEE Trans. Intell. Transp. Syst.*, vol. 15, no. 5, pp. 2040–2048, Oct. 2014.

[7] G. Guo and W. Yue, "Hierarchical platoon control with heterogeneous information feedback," *IET Control Theory Appl.*, vol. 5, no. 15, pp. 1766–1781, Oct. 2011.

[8] F. van Wyk, Y. Wang, A. Khojandi, and N. Masoud, "Real-time sensor anomaly detection and identification in automated vehicles," *IEEE Trans. Intell. Transp. Syst.*, vol. 21, no. 3, pp. 1264–1276, Mar. 2020.

[9] M. Li, Y. Chen, K. Hu, C. Pan, and Z. Mao, "Observer-based decentralized fuzzy control for connected nonlinear vehicle systems," *Nonlinear Dyn.*, vol. 111, no. 8, pp. 7321–7337, Apr. 2023.

[10] Z.-Q. Liu, X. Ge, Q.-L. Han, Y.-L. Wang, and X.-M. Zhang, "Secure cooperative path following of autonomous surface vehicles under cyber and physical attacks," *IEEE Trans. Intell. Veh.*, vol. 8, no. 6, pp. 3680–3691, Jun. 2023.

[11] Z. El-Rewini, K. Sadatsharan, N. Sugunaraj, D. F. Selvaraj, S. J. Plathottam, and P. Ranganathan, "Cybersecurity attacks in vehicular sensors," *IEEE Sensors J.*, vol. 20, no. 22, pp. 13752–13767, Nov. 2020.

[12] Y. Mo and B. Sinopoli, "Secure estimation in the presence of integrity attacks," *IEEE Trans. Autom. Control*, vol. 60, no. 4, pp. 1145–1151, Apr. 2015.

[13] Y. Shoukry, P. Nuzzo, A. Puggelli, A. L. Sangiovanni-Vincentelli, S. A. Seshia, and P. Tabuada, "Secure state estimation for cyber-physical systems under sensor attacks: A satisfiability modulo theory approach," *IEEE Trans. Autom. Control*, vol. 62, no. 10, pp. 4917–4932, Oct. 2017.

[14] W. Ao, Y. Song, and C. Wen, "Distributed secure state estimation and control for CPSs under sensor attacks," *IEEE Trans. Cybern.*, vol. 50, no. 1, pp. 259–269, Jan. 2020.

[15] G. D. Chen, D. Y. Yao, H. Y. Li, Q. Zhou, and R. Q. Lu, "Saturated threshold event-triggered control for multiagent systems under sensor attacks and its application to UAVs," *IEEE Trans. Circuits Syst. I, Reg. Papers*, vol. 69, no. 2, pp. 884–895, Feb. 2022.

[16] G. Chen, Y. Liu, D. Yao, H. Li, and C. K. Ahn, "Event-triggered tracking control of nonlinear systems under sparse attacks and its application to rigid aircraft," *IEEE Trans. Aerosp. Electron. Syst.*, vol. 59, no. 4, pp. 4640–4650, Aug. 2023.

[17] T. Yang and C. Lv, "A secure sensor fusion framework for connected and automated vehicles under sensor attacks," *IEEE Internet Things J.*, vol. 9, no. 22, pp. 22357–22365, Nov. 2022.

[18] G. Chen, Q. Zhou, H. Ren, and H. Li, "Sensor-fusion-based event-triggered following control for nonlinear autonomous vehicles under sensor attacks," *IEEE Trans. Autom. Sci. Eng.*, early access, Dec. 5, 2023, doi: 10.1109/TASE.2023.3337073.

[19] H. Ren, H. R. Karimi, R. Lu, and Y. Wu, "Synchronization of network systems via aperiodic sampled-data control with constant delay and application to unmanned ground vehicles," *IEEE Trans. Ind. Electron.*, vol. 67, no. 6, pp. 4980–4990, Jun. 2020.

[20] H. Luo, I. A. Hiskens, and Z. Hu, "Stability analysis of load frequency control systems with sampling and transmission delay," *IEEE Trans. Power Syst.*, vol. 35, no. 5, pp. 3603–3615, Sep. 2020.

[21] Z. A. Biron, S. Dey, and P. Pisu, "Real-time detection and estimation of denial of service attack in connected vehicle systems," *IEEE Trans. Intell. Transp. Syst.*, vol. 19, no. 12, pp. 3893–3902, Dec. 2018.

[22] J. Zhang, C. Peng, and X. Xie, "Platooning control of vehicular systems by using sampled positions," *IEEE Trans. Circuits Syst. II, Exp. Briefs*, vol. 70, no. 7, pp. 2435–2439, Jul. 2023.

[23] L. Zuo, P. Wang, M. Yan, and X. Zhu, "Platoon tracking control with road-friction based spacing policy for nonlinear vehicles," *IEEE Trans. Intell. Transp. Syst.*, vol. 23, no. 11, pp. 20810–20819, Nov. 2022.

[24] Z. Peng and J. Wang, "Output-feedback path-following control of autonomous underwater vehicles based on an extended state observer and projection neural networks," *IEEE Trans. Syst., Man, Cybern., Syst.*, vol. 48, no. 4, pp. 535–544, Apr. 2018.

[25] R. Cui, L. Chen, C. Yang, and M. Chen, "Extended state observer-based integral sliding mode control for an underwater robot with unknown disturbances and uncertain nonlinearities," *IEEE Trans. Ind. Electron.*, vol. 64, no. 8, pp. 6785–6795, Aug. 2017.

[26] B. Cui, Y. Xia, K. Liu, Y. Wang, and D.-H. Zhai, "Velocity-observer-based distributed finite-time attitude tracking control for multiple uncertain rigid spacecraft," *IEEE Trans. Ind. Informat.*, vol. 16, no. 4, pp. 2509–2519, Apr. 2020.

[27] N. Ali, I. Tawiah, and W. Zhang, "Finite-time extended state observer based nonsingular fast terminal sliding mode control of autonomous underwater vehicles," *Ocean Eng.*, vol. 218, Dec. 2020, Art. no. 108179.

[28] X. Zheng, S. Li, X. Luo, Y. Zhang, X. Li, and X. Guan, "Fast distributed platooning of connected vehicular systems with inaccurate velocity measurement," *IEEE Trans. Syst., Man, Cybern., Syst.*, vol. 53, no. 10, pp. 5996–6006, Oct. 2023.

[29] S. Mondal and S. Sonar, "A fixed time extended state observer based multi leader consensus control for merging and splitting of platoons," *J. Electr. Eng. Technol.*, vol. 19, no. 6, pp. 3765–3779, Feb. 2024.

[30] J. Wang, X. Luo, L. Wang, Z. Zuo, and X. Guan, "Integral sliding mode control using a disturbance observer for vehicle platoons," *IEEE Trans. Ind. Electron.*, vol. 67, no. 8, pp. 6639–6648, Aug. 2020.

[31] J. Wang, X. Luo, J. Yan, and X. Guan, "Distributed integrated sliding mode control for vehicle platoons based on disturbance observer and multi power reaching law," *IEEE Trans. Intell. Transp. Syst.*, vol. 23, no. 4, pp. 3366–3376, Apr. 2022.

[32] C. Pan, Y. Chen, Y. Liu, and I. Ali, "Adaptive resilient control for interconnected vehicular platoon with fault and saturation," *IEEE Trans. Intell. Transp. Syst.*, vol. 23, no. 8, pp. 10210–10222, Aug. 2022.
[33] X.-G. Guo, W.-D. Xu, J.-L. Wang, J. H. Park, and H. Yan, "BLF-based neuroadaptive fault-tolerant control for nonlinear vehicular platoon with time-varying fault directions and distance restrictions," *IEEE Trans. Intell. Transp. Syst.*, vol. 23, no. 8, pp. 12388–12398, Aug. 2022.
[34] Z. Gao, Z. Sun, and G. Guo, "Automatic adjustable fixed-time prescribed performance control of heterogeneous vehicular platoons with actuator saturation," *IEEE Trans. Intell. Transp. Syst.*, vol. 25, no. 9, pp. 12736–12748, Sep. 2024.
[35] Z. Gao, Z. Sun, and G. Guo, "Adaptive predefined-time tracking control for vehicular platoons with finite-time global prescribed performance independent of initial conditions," *IEEE Trans. Veh. Technol.*, vol. 73, no. 11, pp. 16254–16267, Nov. 2024.
[36] Q. Cui, Y. Song, and C. Wen, "Prescribed time consensus control of multiagent systems with minimized time-varying cost function," *IEEE Trans. Autom. Control*, vol. 69, no. 5, pp. 3381–3388, May 2024.
[37] A. Polyakov, "Nonlinear feedback design for fixed-time stabilization of linear control systems," *IEEE Trans. Autom. Control*, vol. 57, no. 8, pp. 2106–2110, Aug. 2012.
[38] Q. Yao, "Semiglobal fixed-time output feedback stabilization for a class of nonlinear systems," *Int. J. Robust Nonlinear Control*, vol. 31, no. 4, pp. 1358–1374, Mar. 2021.
[39] Y. Zheng, S. Eben Li, J. Wang, D. Cao, and K. Li, "Stability and scalability of homogeneous vehicular platoon: Study on the influence of information flow topologies," *IEEE Trans. Intell. Transp. Syst.*, vol. 17, no. 1, pp. 14–26, Jan. 2016.
[40] Y. Liu and H. Gao, "Stability, scalability, speedability, and string stability of connected vehicle systems," *IEEE Trans. Syst., Man, Cybern., Syst.*, vol. 52, no. 5, pp. 2819–2832, May 2022.
[41] V. K. Tripathi, A. K. Kamath, L. Behera, N. K. Verma, and S. Nahavandi, "An adaptive fast terminal sliding-mode controller with power rate proportional reaching law for quadrotor position and altitude tracking," *IEEE Trans. Syst., Man, Cybern., Syst.*, vol. 52, no. 6, pp. 3612–3625, Jun. 2022.
[42] X. Jin, W. M. Haddad, and T. Yucelen, "An adaptive control architecture for mitigating sensor and actuator attacks in cyber-physical systems," *IEEE Trans. Autom. Control*, vol. 62, no. 11, pp. 6058–6064, Nov. 2017.
[43] J. Zhou et al., "Decentralized robust control for vehicle platooning subject to uncertain disturbances via super-twisting second-order sliding-mode observer technique," *IEEE Trans. Veh. Technol.*, vol. 71, no. 7, pp. 7186–7201, Jul. 2022.
[44] H. Zhang, X. Guo, J. Sun, and Y. Zhou, "Event-triggered cooperative adaptive fuzzy control for stochastic nonlinear systems with measurement sensitivity and deception attacks," *IEEE Trans. Fuzzy Syst.*, vol. 31, no. 3, pp. 774–785, Mar. 2023.
[45] X.-M. Li, D. Yao, P. Li, W. Meng, H. Li, and R. Lu, "Secure finite-horizon consensus control of multiagent systems against cyber attacks," *IEEE Trans. Cybern.*, vol. 52, no. 9, pp. 9230–9239, Sep. 2022.
[46] L. Zhang, L. Zhu, C. Hua, and C. Qian, "Fixed-time observer-based output feedback control for nonlinear systems with full-state constraints," *IEEE Trans. Circuits Syst. II, Exp. Briefs*, vol. 71, no. 2, pp. 657–661, Feb. 2024.
[47] Y. Zhao, X. Du, C. Zhou, Y.-C. Tian, X. Hu, and D. E. Quevedo, "Adaptive resilient control of cyber-physical systems under actuator and sensor attacks," *IEEE Trans. Ind. Informat.*, vol. 18, no. 5, pp. 3203–3212, May 2022.

Zhenyu Gao (Member, IEEE) received the Ph.D. degree from Dalian Maritime University, Dalian, China, in 2019.

He is currently an Associate Professor with the School of Control Engineering, Northeastern University at Qinhuangdao. His current research interests include cooperative control of autonomous vehicles and intelligent transportation systems.

Xiang Li received the B.S. degree from Qingdao University of Science and Technology, Qingdao, China, in 2022. He is currently pursuing the M.S. degree with the School of Control Engineering, Northeastern University at Qinhuangdao, Qinhuangdao, China.

His research interests include optimal control, formation control of autonomous vehicles, and intelligent transportation systems.

Zhongyang Wei received the B.S. degree from Shandong University of Science and Technology in 2023. He is currently pursuing the M.S. degree with the School of Control Engineering, Northeastern University at Qinhuangdao.

His research interests include vehicular platoon control and intelligent transportation systems.

Wei Liu received the B.S. degree from Dalian Polytechnic University in 2022. He is currently pursuing the M.S. degree with the School of Control Engineering, Northeastern University at Qinhuangdao.

His research interests include vehicular platoon control and intelligent transportation systems.

Ge Guo (Senior Member, IEEE) received the B.S. and Ph.D. degrees from Northeastern University, Shenyang, in 1994 and 1998, respectively.

He is currently a Professor with Northeastern University (NEU) and the Director of the Center of Intelligent Transportation Systems, NEU. He has published over 200 international journal articles. His research interests include intelligent transportation systems and cyber-physical systems.

Prof. Guo won a series of awards, including the CAA Young Scientist Award, the First Prize of Natural Science Award of Hebei Province, and the First Prize of Science and Technology Progress Award of Gansu Province. He is an Associate Editor of IEEE TRANSACTIONS ON INTELLIGENT TRANSPORTATION SYSTEMS, IEEE TRANSACTIONS ON VEHICULAR TECHNOLOGY, IEEE TRANSACTIONS ON INTELLIGENT VEHICLES, *Information Sciences*, *IEEE Intelligent Transportation Systems Magazine*, *ACTA Automatica Sinica*, *China Journal of Highway and Transport*, and the *Journal of Control and Decision*.

Shixi Wen (Senior Member, IEEE) received the M.E. and Ph.D. degrees in control science and control engineering from Dalian Maritime University, Dalian, China, in 2011 and 2015, respectively.

He is currently an Associate Professor with Dalian University, Dalian. His research interests include networked control systems and vehicular cooperative control in intelligent vehicle highway systems.